Journal of Neuroscience Methods 206 (2012) 1–6

Contents lists available at SciVerse ScienceDirect

Journal of Neuroscience Methods

journal homepage: www.elsevier.com/locate/jneumeth

Basic Neuroscience
Short communication

Reconstruction of field excitatory post-synaptic potentials in the dentate gyrus from amperometric biosensor signals

Alessandro Viggiano[a,*], Stéphane Marinesco[b], Frédéric Pain[a], Anne Meiller[c], Hirac Gurden[a]

[a] CNRS UMR8165, Imagerie et Modélisation en Neurobiologie et Cancérologie, Université Paris Diderot 7, Paris Sud 11, Orsay F-91405, France
[b] INSERM U1028; CNRS UMR5292 Lyon Neuroscience Research Center, Integrated Physiology of the Waking State, Lyon F-69000, France
[c] Plate-forme technologique AniRA-NeuroChem, INSERM U1028 Lyon Neuroscience Research Center, University Lyon 1, Lyon F-69000, France

ARTICLE INFO

Article history:
Received 8 December 2011
Received in revised form 24 January 2012
Accepted 25 January 2012

Keywords:
Amperometry
Biosensor
Electrode model
Evoked potential reconstruction
LTP

ABSTRACT

A new feasible and reproducible method to reconstruct local field potentials from amperometric biosensor signals is presented. It is based on the least-square fit of the current response of the biosensor electrode to a voltage step by the use of two time constants. After determination of the electrode impedance, Fast Fourier Transform (FFT) and Inverse FFT are performed to convert the recorded amperometric signals into voltage and trace the local field potentials using a resistor–capacitor circuit-based model. We applied this method to reconstruct field evoked potentials from currents recorded by a lactate biosensor in the rat dentate gyrus after stimulation of the perforant pathway *in vivo*. Initial slope of the reconstructed field excitatory postsynaptic potentials was used in order to demonstrate long term potentiation induced by high frequency stimulation of the perforant path.

Our results show that reconstructing evoked potentials from amperometric recordings is a reliable method to obtain *in vivo* electrophysiological and amperometric information simultaneously from the same electrode in order to understand how chemical compounds vary with and modulate the dynamics of brain activity.

1. Introduction

Neurotransmission is electrochemical in nature. Therefore information about biochemical dynamics underlying brain activity is essential for our understanding of brain physiology. Biosensors based on amperometric methods are unique tools which make possible the study of real-time changes in the interstitial concentrations of neurotransmitters and energetic molecules on the time scale of seconds or less. In order to monitor extracellular molecular contents and probe neuronal activity at the same time, a promising research direction is the acquisition of electrophysiological and neurochemical information from a biosensor in the same preparation simultaneously (Zhang et al., 2009, 2010).

Amperometric signals used in biosensor approaches result from the currents due to chemical oxidation or reduction when a voltage is applied to the same microelectrode that is used to measure the current (Marinesco and Pernot, 2008). Interestingly, high frequency components of these amperometric signals can give information about local field potentials (LFPs) as they have similar spectral fluctuations (Zhang et al., 2009). However, conversion from the high frequency components of amperometric signals to conventional LFP is a challenging task since (i) the electrode impedance is difficult to determine and the electrical properties of microelectrodes appear to change with the frequency (Robinson, 1968) and (ii) an electrode–electrolyte interface is a nonlinear circuit element that can be operated over a wide frequency and current density range. Yet, under specified operating conditions, it may be possible to create an adequate electrode model to convert the recorded currents into voltage (Geddes, 1997): for example, a resistor–capacitor (*RC*) circuit of passive elements with 2 time constants fits well the electrophysiological experimental data as shown for the capacitive currents of cell membrane (Ildefonse and Rougier, 1972). To our knowledge, despite its simplicity (the element values are not function of the frequency), this *RC*-based electrode model and its possible fields of application were not further investigated (de Boer and van Oosterom, 1978).

In this study, we applied an *RC*-based electrode model to characterize the electrical properties of platinum electrodes and biosensors. We reliably reconstructed the evoked potentials (EPs) from the currents recorded with a lactate biosensor and elicited in the dentate gyrus of rats by stimulation of the perforant pathway.

* Corresponding author. Current address: Second University of Naples, Department of Experimental Medicine (Section of Human Physiology), Via Costantinopoli, 16-80138 Naples, Italy. Tel.: +33 1 69 15 36 44.
E-mail address: alessandro.viggiano@unina2.it (A. Viggiano).

0165-0270/$ – see front matter © 2012 Elsevier B.V. All rights reserved.
doi:10.1016/j.jneumeth.2012.01.013

We then induced long term potentiation (LTP) of synaptic efficacy in the dentate gyrus by applying high frequency stimulation of the perforant path and demonstrated the occurrence of LTP through quantitative measures of the reconstructed EPs.

2. Materials and methods

2.1. Animals

Four Long–Evans rats (body weight, 300–450 g) were used for this study. They were housed at constant conditions of temperature (21 ± 2 °C) and humidity (45–55%) with a 24 h light cycle (light on at 8.00 AM, off at 8.00 PM). All experiments were conducted according to European Community Council (EEC) guidelines and directives (86/09/EEC).

2.2. Biosensor preparation

Biosensors were prepared as previously described (Pernot et al., 2008; Vasylieva et al., 2011). Briefly, platinum electrodes were constituted of a 25 μm diameter 90% platinum/10% iridium wire (Goodfellow, Huntington, UK) glued to a 0.3 mm copper wire using electroconductive silver paint (Radiospares, Beauvais, France). They were then inserted into a pulled glass capillary (Harvard Apparatus, Edenbridge, UK), and the tip of the pipet was cut to let about 100 μm of the platinum wire protrude out of the glass. The junction between the platinum wire and the pipette tip was sealed by locally melting the glass. The junction between the copper wire and the glass was sealed with epoxy resin (Araldite, Bostik, Paris, France).

The electrodes were then washed for 30 min in 0.5 M KOH and 20 min in ethanol. A poly-m-phenylenediamine (PPD) layer was electrodeposited by dipping the electrodes for 20 min in a solution containing 100 mM m-phenylenediamine in 0.01 M phosphate-buffered saline (PBS) at pH 7.4 under a constant potential of +700 mV *versus* an Ag/AgCl reference electrode. The enzyme layer was deposited by dipping the platinum tip of the electrodes in a lactate oxidase solution composed of 60 mg/mL of lactate oxidase, 30 mg/mL bovine serum albumin (BSA), 2% glycerol and 60 mg/mL poly(ethylene glycol) diglycidyl ether (PEGDE) in PBS 0.01 M (pH 7.4). The enzyme was immobilized after 2 h at 55 °C (Vasylieva et al., 2011). Electrodes were then kept at −20 °C in dry atmosphere for long-term storage.

2.3. Electrophysiological setup

Constant potential amperometry was performed with an electrochemistry amplifier VA-10 (NPI Electronics, Tamm, Germany) used with a two-electrode potentiostat. Signals were digitalized through the CED Power1401 mk II (Cambridge Electronic Design, Cambridge, England) and stored on the hard disk. Spike2 software (CED, England) was used to control acquisition and to perform real time analysis. The oxidation current was filtered (0–300 Hz), sampled at 2 kHz and averaged over 2000 data points, yielding a final sampling frequency of 1 Hz. Triggered acquisition of unfiltered signal was performed at 100 kHz (for fitting the current response to a voltage square pulse) or at 20 kHz (for reconstruction of EPs). Offline analysis was performed through labVIEW (National Instruments) and MATLAB (MathWorks) softwares.

Voltage recordings (bandpass 0.1–10,000 Hz) were done through AC amplifier P511 (Grass Technologies Inc, USA). Signals were digitalized at 20 kHz.

2.4. Electrode model and current to voltage conversion

The equivalent *RC* circuit previously described by Ildefonse and Rougier (Ildefonse and Rougier, 1972) is shown in Fig. 1A.

The current response of this model to the rise (or the fall) of a voltage step obeys to the equation:

$$i(t) = V_0 \left(\frac{1}{R_1} \exp\left(\frac{-t}{R_1 C_1}\right) + \frac{1}{R_2} \exp\left(\frac{-t}{R_2 C_2}\right) + \frac{1}{R_3} \right)$$

where V_0 is the imposed potential.

The resistances (R_1, R_2, R_3) and capacitances (C_1, C_2) values of the circuit were therefore estimated by fitting the current response to a voltage step of few millivolts.

For a sinusoidal signal, the impedance Z_1 of the arm R_1C_1 and the impedance Z_2 of the arm R_2C_2 can be calculated as: $Z_1 = R_1 + \frac{1}{j\omega C_1}$ and $Z_2 = R_2 + \frac{1}{j\omega C_3}$ where j is the imaginary unit and ω is the angular frequency of the sinusoidal signal. The overall impedance Z of the circuit shown in Fig. 1A is then:

$$Z = \frac{Z_1 Z_2 R_3}{Z_1 R_3 + Z_2 R_3 + Z_1 Z_2}$$

For offline conversion of the EPs from current to voltage signal, the recordings in current were converted to frequency domain through FFT, multiplied for the impedance and transformed back to the time domain with inverse FFT.

2.5. In vitro experiments

Platinum electrodes and biosensors responses for different voltage pulses at different holding potentials (0, +200 and +500 mV with respect to the reference) were tested in PBS. For each combination of electrode, holding potential and voltage pulse (see Fig. 1D), a single estimation of the least squares set of 5 coefficients that best fit the set of recorded points was done by the Levenberg–Marquardt algorithm. Since different electrodes were expected to differ in the basal values of R_1, C_1, R_2, C_2, R_3, the values obtained from each electrode in different conditions of pulse and holding potential were expressed as *z*-score (*e.g.*, mean and standard deviation of R_1 in biosensor 2 were calculated over the 6 estimations of R_1 values; then *z*-score of these values was calculated as (value − mean)/standard deviation). *R*-square for non-linear fit was calculated in order to assess goodness of fit. Results were expressed as mean ± standard error of the mean (SEM).

2.6. In vivo electrophysiology

Animals were anesthetized with intraperitoneal (i.p.) injection of urethane. Initially, they received 1.0 g/kg and further increments, if required, to get absence of response to tail pinch (maximum total doses was 1.6 g/kg). The body temperature was monitored by a rectal thermometer and maintained at 37.0 °C by an electrically shielded heating pad. Two small holes were drilled into the skull to target the perforant pathway for electrical stimulation and the hilus of the dentate gyrus for EP recordings. The shape of this EP trace is typically characterized by a large positive wave (fEPSP) with a superimposed negative wave (population spike (PS)). The following stereotaxic coordinates were used: 2.2 mm lateral and 3.5 mm posterior to Bregma for the recording electrode; 4.4 mm lateral and 8.0 mm posterior to Bregma for the concentric bipolar stimulating electrode (Paxinos and Watson, 2007). Depth of these electrodes was optimized online to get the best EP shape (dorsoventral coordinates range from brain surface: 3.0–3.2 mm for the recording electrode and 2.9–3.3 mm for the stimulating electrode). Stimulation electrodes were made of insulated stainless steel wire (Ø 75 μm protruding about 500 μm from a stainless steel tube, Ø 457 μm).

At about 2 mm from brain surface, the biosensor current response to a voltage step (<2 mV) was recorded to make the current to voltage conversion possible after electrodes implantation

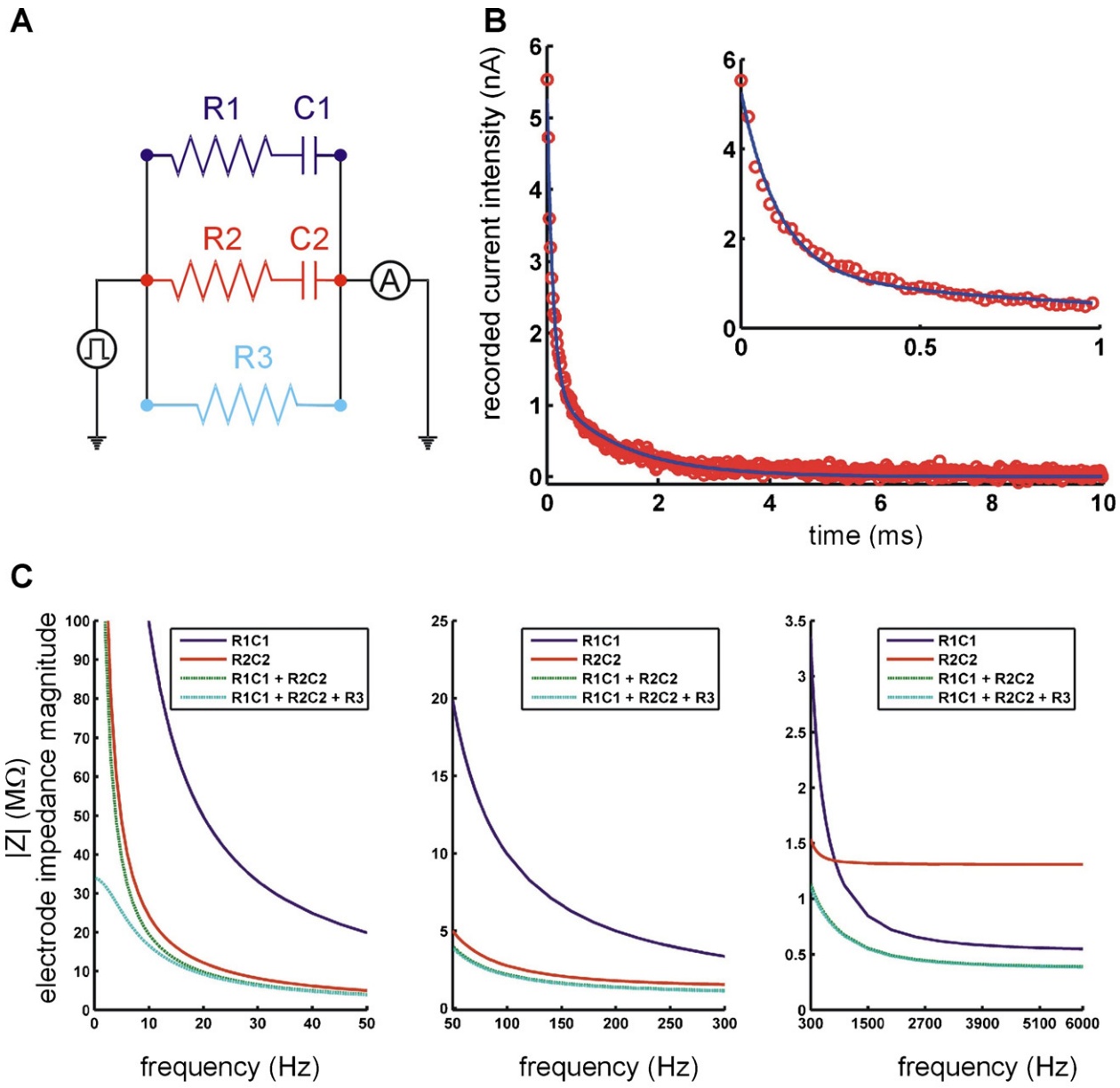

D

	Holding potential		
	0 mV	200 mV	500 mV
	Voltage pulse (mV)		
biosensor 1	1.0	1.0	1.0, 2.0
biosensor 2	1.0, 2.0	1.0, 2.0	1.0, 2.0
biosensor 3	0.5, 0.8	0.5, 0.8	0.5, 0.8
bare electrode	0.3, 0.5	0.3, 0.5	0.3, 0.5

E

	R1 (MΩ)	C1 (nF)	R2 (MΩ)	C2 (nF)	R3 (MΩ)
biosensor 1	0.65	1.32	0.26	0.32	16.9
biosensor 2	0.85	1.10	0.32	0.15	15.8
biosensor 3	0.46	1.32	0.24	0.36	24.6
bare electrode	0.31	1.73	0.049	1.89	15.7

Fig. 1. A resistor–capacitor (*RC*)-based circuit as an electrode model. (A) The equivalent *RC* circuit proposed to explain the time course observed in the current recordings from the electrode of our biosensors: a voltage pulse produced by a rectangular waveform generator produces a current *i*, sum of the current i_1, i_2 and i_3 that circulate in each arm of the circuit. [*A*] represents the current recording system. (B) Example (biosensor 1, 500 mV holding potential, 1 mV voltage step) of data fitting on a period of 10 ms. Inset represents the time course of the recorded current during the first ms. (C) Impedance magnitude (|*Z*|) analysis of data obtained by the curve in (B): the higher the |*Z*| value of each arm of the circuit in (A), the lower its contribution in the overall |*Z*| of the circuit. At very low frequency (<10 Hz), the theoretical circuit impedance approaches the one of R_3. At low frequency (20–200 Hz), the circuit series R_1C_1 gives the highest contribution to the total impedance and only for higher frequency the contribution of the series R_2C_2 becomes relevant. To clearly visualize the dynamics of impedance magnitude in response to the three frequency ranges, the MΩ scale was maximized for each of the three panels in (C). (D) *In vitro* test conditions for the 4 electrodes. For each combination of electrode/holding potential/voltage pulse, a single estimation of the least squares of 5 coefficients that best fit the recorded points was done by the Levenberg–Marquardt algorithm. (E) *In vitro* estimation of model parameters for each electrode at 500 mV holding potentials. Each value is the mean of two measurements at two different voltage pulses.

in the brain. Recordings were performed at constant holding potential of +500 mV. In order to induce LTP in rats, electrodes depths were adjusted to maximize the slope of the fEPSPs. The animals were allowed to recover for 1 h after electrode implantation. After this time, an input–output curve was obtained with ascending–descending series of 6–10 stimulation intensities, covering a range of responses from subthreshold to supramaximal. The curve was fitted using a Boltzman equation. The stimulation intensity which evoked a fEPSP at 50% of its maximal slope was chosen for the test pulses and for the tetanus. Square pulses (50 μs) were given at 30 s interval from 15 min before and 60 min after a high frequency stimulation (3 trains of stimuli 30 s apart; 50 pulses at 250 Hz) (Viggiano et al., 2006). The responses were quantified by the analysis of the slope (on the first 0.5 ms of the rising phase) of fEPSPs. Results were expressed as percentage of the pretetanus mean value of fEPSP slope ± SEM.

Before retracting the electrodes, the biosensor current response to a voltage step was again recorded in order to check the stability of the electrode properties over the time.

3. Results

In order to characterize the reliability of our model for voltage reconstruction, a set of *in vitro* experiments was conducted to determine goodness of model prediction for fast voltage changes and for different holding potentials. The equivalent *RC* circuit of the electrode was modeled as three resistances and two capacitances arranged in three parallel arms (Fig. 1A). The behavior of these elements was explored *in vitro* by testing the response of lactate biosensors *versus* a control electrode. 4 electrodes (1 bare platinum as a control, 3 electrodes covered by lactate oxidase) were used to test their responses to square pulses of different amplitudes at different holding potentials (Fig. 1B). The mean *R*-square ± SEM of the least-square fitting of the first 10 ms in 22 responses was 0.981 ± 0.003. The use of four elements (R_1, C_1, R_2, C_2) instead of 5 significantly decreased the mean *R*-square values of the fitted responses for the 3 electrodes covered by the enzyme (paired *t* test; $p < 0.01$) but not for the bare platinum electrode. The time decay constants of the *RC* series was 0.662 ± 0.048 ms and 0.071 ± 0.005 ms respectively in the first (R_1, C_1) and the second arm (R_2, C_2) of the circuit. Their ratio ranged between 5 and 23. At low frequency (20–200 Hz), the circuit series R_1C_1 gave the highest contribution to the total impedance (magnitude) and only for higher frequency the contribution of the series R_2C_2 became relevant. At very low frequency (<10 Hz), the theoretical circuit impedance approached the one of R_3 (Fig. 1C). A two-way random effects ANOVA (pulse intensity × holding potentials) showed that there was no significant effect of pulse intensity (range 0.3–2.0 mV) or of the interaction pulse intensity × holding potentials on the values of the circuit elements. On the contrary, holding potentials (0, 200 and 500 mV) had a significant effect on C_1 ($F(2,7) = 67.88$; $p < 0.01$), C_2 ($F(2,6) = 11.21$; $p < 0.05$) and R_3 ($F(2,6) = 28.57$; $p < 0.01$). *Post hoc* test revealed that these values were significantly lower at 0 mV holding potential than at 200 and 500 mV holding potentials. *In vitro* test conditions are shown in Fig. 1D, parameters estimations at 500 mV holding potential are shown in Fig. 1E. Overall these results show that *in vitro* the model has good prediction and reliability at constant holding potentials.

Following the *in vitro* characterization of our model, we moved to *in vivo* recordings of currents from lactate biosensors. We applied our *RC*-based model to these amperometric signals (Fig. 2A and B) and reconstructed EPs in the dentate gyrus of the hippocampus in response to perforant path stimulation (Fig. 2C). After stabilization of DC baseline (about 30 min after electrode insertion), changes in the parameters estimated before and after the recording period (75 min) were negligible. The mean of 10 reconstructed EPs was compared with the mean of 10 EPs collected with an AC amplifier after disconnecting of the amperometric amplifier without moving the electrodes (Fig. 2D). In the rat molecular layer of dentate gyrus (Fig. 2D1), the reconstructed voltage waveform clearly reproduced the shape of the actual voltage recording: it was composed by a large negative wave (fEPSP) with a superimposed positive spike (PS). In the hilus (Fig. 2D2), the reconstructed voltage waveform showed as expected a large positive fEPSP with a superimposed negative PS. Quantitative measures of reconstructed EPs were carried out and compared to actual voltage recordings. In the molecular layer, the mean fEPSP slope was 5.28 ± 0.05 (mV/ms) and the mean PS amplitude was 1.73 ± 0.02 mV. Accuracy of these two measures was respectively 90% and 85%. In the hilus, the mean fEPSP slope was 6.07 ± 0.03 (mV/ms) with an accuracy of 90% and mean amplitude of PS was 4.28 ± 0.06 mV with an accuracy of 97%. Precision of all the estimated parameters was not different between reconstructed and actual voltage waveforms (Levene's test for equality of variances not significant).

In addition, depth profile of the reconstructed responses also showed the typical inversion of the wave polarity when the electrode crossed the granular layer (Fig. 2E).

LTP was induced reliably in 4 rats by 3 trains of 50 pulses at 250 Hz. 60 min following high frequency stimulation, the mean slope percentage increase of the fEPSP was 136 ± 10 with respect to the baseline (Fig. 2F).

4. Discussion

In this study we built a simple *RC*-based circuit model to characterize electrode properties and consequently reconstruct LFP from the amperometric signals of our biosensors. A reliable circuit model for the electrode–electrolyte interface represents a challenge and likely there is no single model which could account for all the electrical properties seen in different electrodes and in different recording conditions (Chang et al., 2007; Geddes, 1997). Our results showed that for specific electrophysiological purposes, as the LFP recordings in the dentate gyrus in the present study, a relatively simple *RC*-based model characterizing electrode properties can satisfactorily work to transform recorded currents into voltage, then to reconstruct LFP traces.

We adopted a model characterized by 5 variables. Their values could be determined through the least-square fitting of a single square voltage pulse. When the holding potential approached 0 there was a significant effect on model variables values with respect to the values determined at 200 mV and 500 mV holding potentials. The relevance of this effect might preclude the use of our model in conditions where the holding potential crosses the zero as in cyclic voltammetry. On the contrary, in constant potential amperometry, the model variables values were stable and small voltage pulses (maximum 2 mV in the present study) did not affect significantly those values. Even if the amplitude of the EPs recorded in the dentate gyrus can be even greater than 10 mV, the current peak recorded during EPs is smaller than the one produced by the square pulses tested *in vitro*. Therefore the voltage changes represented by the EPs are not expected to modify the characteristics of the equivalent circuit.

The equivalent electrical circuit we used to model the electrode was previously proposed in a different field by Ildefonse and Rougier (1972) to study the capacitive current in the frog skeletal muscle fiber preparation. The introduction of two time constants to describe the response to a voltage step gives also the chance to discard one of them if its contribution to total impedance is small

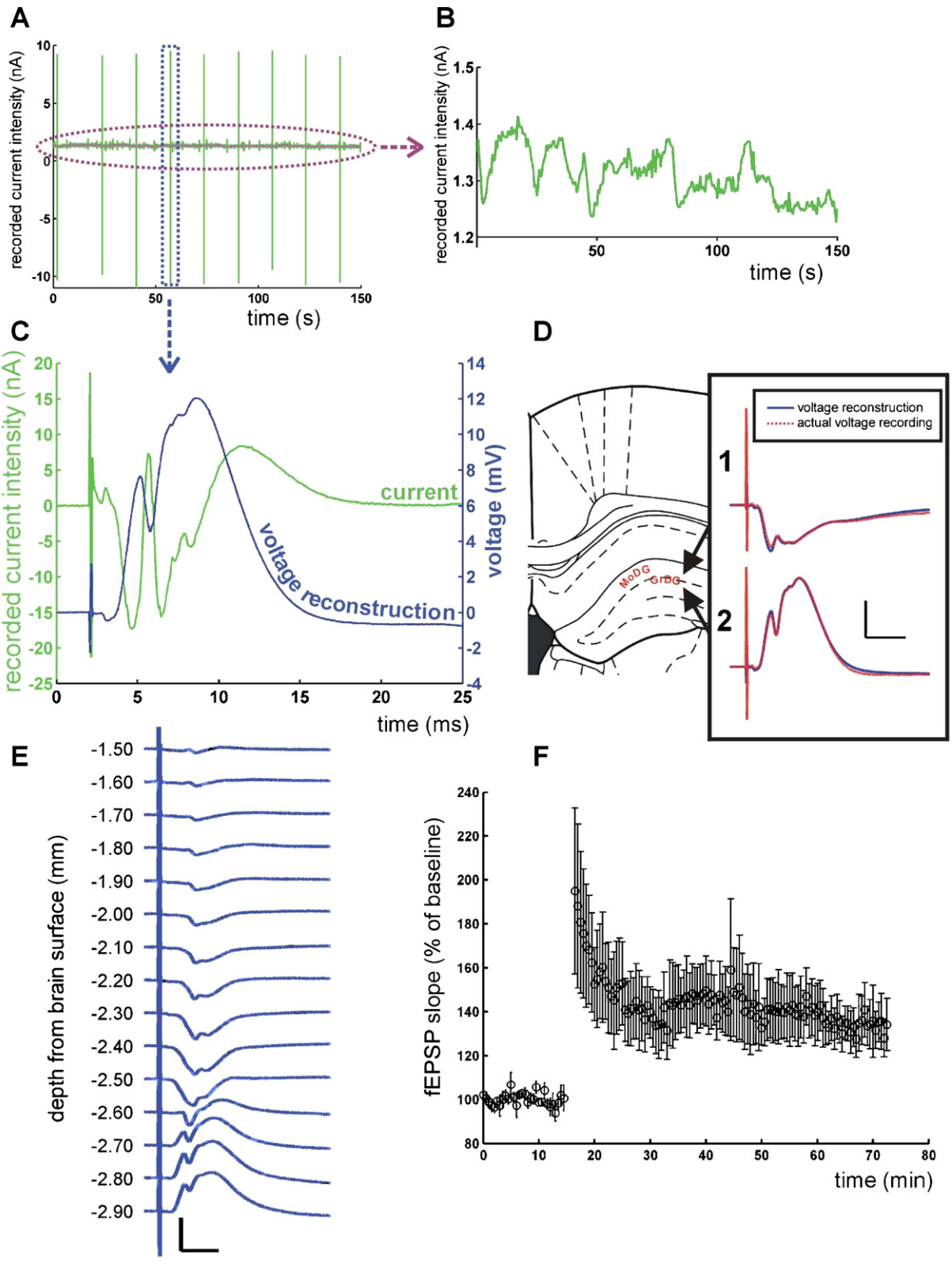

Fig. 2. Simultaneous acquisition of electrophysiological and neurochemical information from the same current recording. (A) *In vivo* amperometric signal from the biosensor sampled at 2 kHz. Evoked potential (EP) events (blue dash line) are present as high amplitude, high frequency components. (B) Mean signal from A over 0.5 s epochs reflecting fluctuations in extracellular lactate concentration. (C) Triggered acquisition of 200 ms epochs sampled at 20 kHz to store EPs and allow reconstruction of voltage waveforms. (D) Example of reconstructed EP (blue) overlapping the actual voltage recordings (red) at different depths in the rat dentate gyrus (1 = molecular layer; 2 = hilus). Each trace is a band representing the mean ± SEM of 10 EPs. Note the perfect overlapping of the traces and precision (error is often smaller than the linewidth) with the characteristic large positive wave (fEPSP) with a superimposed negative wave (population spike). (E) Reconstructed EPs recorded at different depths in the rat hippocampus. Note the typical waveform inversion as the electrode crosses the granular layer. (F) LTP induction in the rat dentate gyrus. Slope of the reconstructed EPs was recorded 15 min before and 60 min after high frequency stimulation. Data are expressed as mean ± SEM ($n = 4$). the mean slope increase of the fEPSP was 136 ± 10% with respect to the baseline. Calibration bars in (D) and (E) are 5 mV vertically, 5 ms horizontally.

in the frequencies of interest. In our biosensors, one of the two time constant was 5–23 times smaller than the second one. The introduction of two time constants to describe the response to a voltage step gives also the chance to discard one of them if its contribution to total impedance is negligible in the frequencies of interest or if only qualitative aspects of the signal are of interest (*e.g.*, in the electrophysiological guide for electrode positioning). In that case the conversion formula becomes simple as:

$$V(t) = i_t R + \frac{1}{C}\int i_t\, dt$$

Offline analysis from *in vivo* data allowed demonstrating all the characteristics of actual voltage recordings. Interestingly, reconstruction showed: (i) positive large waveforms with superimposed negative spike in the hilus of dentate gyrus, (ii) inversion of polarity when the electrode crosses the granular layer, (iii) amplitude and shape of the reconstructed EPs comparable to the ones of an actual voltage recordings. Finally, common measures of the EPs in dentate gyrus could be successfully achieved to the purpose of showing LTP. An important aspect of our method is that the parameters estimation of the *RC*-based model in the *in vivo* recordings was done by the application of with a small voltage pulse ($\leq$2 mV) to the *in vivo* preparation. In fact, due to possible different conductivity properties of different media, parameters estimated *in vitro* could be not appropriate for *in vivo* recordings.

Previous studies tried to model the impedance behavior of metal microelectrodes (Block, 1968; de Boer and van Oosterom, 1978; Geddes, 1997; Onaral and Schwan, 1982, 1983; Robinson, 1968; Schwan and Onaral, 1985). De Boer & van Oosterom provided interesting equations for a time-domain analysis of the electrical properties of metal microelectrodes (de Boer and van Oosterom, 1978). Their equation to fit the current response of the electrode to a voltage step needs adaptation when applied for step >1–2 ms and therefore it has some practical limits. Moreover, they did not furnish a physical explanation for their model.

The electrical equivalent circuit of our model is made by three arms connected in parallel. Two arms have capacitive behavior while the third one is a pure resistance. Interestingly, our biosensor electrode has two compartments that in theory could show a capacitive behavior and can be translated as follows in terms of interfaces. The first one is the metal–electrolyte interface under the form of an electric double layer due to the electrode polarization (Robinson, 1968). The second one is represented by the interface platinum–glass–electrolyte at the tip of the electrode where two conductive surfaces (platinum inside and electrolytes outside the electrode) are separated by thin glass. This second putative capacitor would be in parallel to the first one. The third arm represented by one single resistance could be due to the presence of the enzyme layer. Accordingly to this description, the *R*-square of the least-square fitting of electrode responses decreased in the absence of R_3 in the model for the electrode covered by the enzyme but it does not change significantly for a bare platinum electrode insulated with glass.

To conclude, we presented and validated a feasible and reproducible method to reconstruct LFPs from amperometric biosensor signals. Such a method promises to be an important tool for combining amperometric neurochemistry with extracellular electrophysiological recordings. Extensions of the method to the purpose of reconstructing long LFP recordings in acute preparation and in chronically implanted biosensor electrodes in freely moving animals are under study.

Acknowledgments

This work was supported by the "Agence Nationale de la Recherche" (ANR-09-JCJC-0117-01). We are thankful to Dr. Claire Martin for support in the electrophysiological experiments.

References

Block MT. The electrical and biological properties of tungsten microelectrodes. Med Biol Eng Comput 1968;6:517–25.
Chang J, Park J, Pak YK, Pak JJ. Fitting improvement using a new electrical circuit model for the electrode–electrolyte interface. In: 3rd international IEEE/EMBS conference on neural engineering; 2007. p. 572–4.
de Boer RW, van Oosterom A. Electrical properties of platinum electrodes: impedance measurements and time-domain analysis. Med Biol Eng Comput 1978;16:1–10.
Geddes LA. Historical evolution of circuit models for the electrode–electrolyte interface. Ann Biomed Eng 1997;25:1–14.
Ildefonse M, Rougier O. Voltage-clamp analysis of the early current in frog skeletal muscle fibre using the double sucrose-gap method. J Physiol 1972;222:373–95.
Marinesco S, Pernot P. Biocapteurs implantables in vivo. In: Techniques de l'Ingénieur. RE-108; 2008. p. 1–13.
Onaral B, Schwan HP. Linear and nonlinear properties of platinum electrode polarisation. Part 1: Frequency dependence at very low frequencies. Med Biol Eng Comput 1982;20:299–306.
Onaral B, Schwan HP. Linear and nonlinear properties of platinum electrode polarisation. II: Time domain analysis. Med Biol Eng Comput 1983;21:210–6.
Paxinos G, Watson C. The rat brain in stereotaxic coordinates. 6th ed. Academic Press; 2007.
Pernot P, Mothet JP, Schuvailo O, Soldatkin A, Pollegioni L, Pilone M, Trs Adeline M, Cespuglio R, Marinesco Sp. Characterization of a yeast D-amino acid oxidase microbiosensor for D-serine detection in the central nervous system. Anal Chem 2008;80:1589–97.
Robinson D. The electrical properties of metal microelectrodes. Proc IEEE 1968;56:1065–71.
Schwan HP, Onaral B. Linear and nonlinear properties of platinum electrode polarisation. III: Equivalence of frequency- and time-domain behaviour. Med Biol Eng and Comput 1985:28–32.
Vasylieva N, Barnych B, Meiller A, Maucler C, Pollegioni L, Lin JS, Barbier D, Marinesco S. Covalent enzyme immobilization by poly(ethylene glycol) diglycidyl ether (PEGDE) for microelectrode biosensor preparation. Biosens Bioelectron 2011.
Viggiano A, Viggiano A, Monda M, Turco I, Incarnato L, Vinno V, Viggiano E, Baccari ME, De Luca B. Annurca apple-rich diet restores long-term potentiation and induces behavioral modifications in aged rats. Exp Neurol 2006;199:354–61.
Zhang H, Lin SC, Nicolelis M. Spatiotemporal coupling between hippocampal acetylcholine release and theta oscillations in vivo. J Neurosci 2010;30:13431–40.
Zhang H, Lin SC, Nicolelis MAL. Acquiring local field potential information from amperometric neurochemical recordings. J Neurosci Methods 2009;179:191–200.